

Quantum Chameleons

Philippe Brax,^a Sylvain Fichet^{b,c*}

^a*Institut de Physique Théorique, Université Paris-Saclay,
CEA, CNRS, F-91191 Gif/Yvette Cedex, France*

^b*Walter Burke Institute for Theoretical Physics, California Institute of Technology, Pasadena, CA 91125, California, USA*
^c*ICTP-SAIFR & IFT-UNESP, R. Dr. Bento Teobaldo Ferraz 271, São Paulo, Brazil*

We initiate a quantum treatment of chameleon-like particles, deriving classical and quantum forces directly from the path integral. It is found that the quantum force can potentially dominate the classical one by many orders of magnitude. We calculate the quantum chameleon pressure between infinite plates, which is found to interpolate between the Casimir and the integrated Casimir-Polder pressures, respectively in the limits of full screening and no screening. To this end we calculate the chameleon propagator in the presence of an arbitrary number of one-dimensional layers of material. For the Eöt-Wash experiment, the five-layer propagator is used to take into account the intermediate shielding sheet, and it is found that the presence of the sheet enhances the quantum pressure by two orders of magnitude. As an example of implication, we show that in both the standard chameleon and symmetron models, large and previously unconstrained regions of the parameter space are excluded once the quantum pressure is taken into account.

INTRODUCTION

A wealth of Dark Energy models involve a scalar field with an extremely low mass which plays a role on cosmological scales [1], explaining the accelerated expansion of the Universe. At shorter distances, such as the Solar System scale, screening mechanisms must take place to suppress the long-range force induced by the new scalar, since such scenario would be otherwise excluded by stringent experimental tests [2, 3]. Screening mechanisms of the long-range force can naturally occur as a result of the scalar coupling to matter. Indeed, whenever the local matter density is high enough with respect to the other scales of the problem, the properties of the scalar (mass or couplings) tend to change in the local environment and, typically, the scalar tends to get invisible where one could observe it [4–7]. We will refer to any scalar with such property as a *chameleon-like* field (and will sometimes use only “chameleon” for short). For instance for the original chameleon model the mass of the field increases in dense environments whilst in the symmetron model [8–10] screening occurs as the coupling to matter decreases with an increasing matter density. The existence of chameleon-like fields can be tested by laboratory experiments, for instance by neutrons [11–14] or atomic spectroscopy [15, 16]. The pressure between two parallel plates is also suited to test the potential presence of chameleons [17, 18] which could become within reach in the near future [19].

The effects of chameleon-like fields are typically treated in a classical approximation. However at short enough distances – such as the submicron scale in the Eöt-Wash experiment [20], a quantum treatment of the chameleon mechanism becomes mandatory. In this work we develop the formalism to describe “quantum chameleons” and present some of its consequences. The formalism also sheds new light on the quantum field theory calculation

of the Casimir pressure in its various regimes.

CHAMELEON FORCES FROM THE PATH INTEGRAL

We start with the general chameleon Lagrangian

$$\mathcal{L}[\phi, J] = \frac{1}{2}(\partial_\mu\phi)^2 - V(\phi) - A(\phi)J, \quad (1)$$

where $V(\phi)$ is the interaction potential, J is a source and $A(\phi)J$ describes how the chameleon couples to the source [21]. In this letter J is always considered as a matter density *i.e.* $J(x) = \rho(x)$, is assumed to be static and vanishes at infinity. In general J , ϕ , $A(\phi)$ depend on space. Both V and A can contain higher dimensional operators, in which case the Lagrangian describes a low-energy effective field theory (EFT). In the following we define the effective potential $V_J = V + AJ$.

The source is assumed to depend on an external parameter L , to be understood typically as measuring the distance between two objects. We will study how the quantum system reacts when changing L . To this end we consider the generating functional of connected chameleon correlators

$$W[J] = i \log Z[J], \quad Z[J] = \mathcal{D}\phi e^{i \int d^4x \mathcal{L}[\phi, J]}. \quad (2)$$

When the source is static the vacuum energy is given by $E[J] = \frac{W[J]}{T}$ where $T = \int dt$. We will work with $T = 1$ conventionally and refer to the generating functional directly as the vacuum energy.

All the information about the force (or pressure) that one source induces on another one in the presence of the chameleon-like field is contained in the variation of the vacuum energy with respect to L . This variation is given by

$$\partial_L E[J] = \int d^4x \partial_L J \langle A \rangle. \quad (3)$$

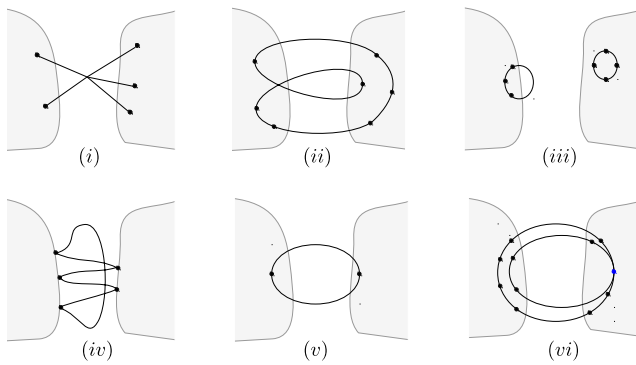


FIG. 1. Sample Feynman diagrams for a chameleon field in the presence of two extended sources. (i): A generic classical contribution. (ii): A generic 1-loop contribution. (iii): Tadpoles. (iv): Casimir (Strong coupling to sources.) (v): Casimir-Polder (Weak coupling to sources.) (vi): A two-loop contribution from higher-dimensional coupling to matter.

The calculation of the quantum average $\langle A \rangle$ is highly non-trivial and can in general be evaluated only in the loop expansion of quantum field theory. Writing the chameleon field as $\phi = \phi_{\text{cl}} + \eta$ where η represents the quantum fluctuations around the classical field ϕ_{cl} , we find the first two terms in the \hbar expansion to be

$$\begin{aligned} \partial_L E &= \int d^4x \partial_L J A(\phi_{\text{cl}}) + \frac{1}{2} \int d^4x \partial_L J A'' \Delta_J(x, x) + O(\hbar^2) \\ &= F_{\text{cl}} + F_{\text{quant}} + O(\hbar^2), \end{aligned} \quad (4)$$

where $\Delta_J(x, x')$ is the Feynman propagator of the fluctuation, which satisfies the equation of motion

$$(\partial_x^2 + V'' + A''J)\Delta_J(x, x') = -i\delta^{(4)}(x - x'), \quad (5)$$

where $V'' = \delta^2 V / \delta^2 \phi_{\text{cl}}$, $A'' = \delta^2 A / \delta^2 \phi_{\text{cl}}$. The convention adopted here is that $F > 0$ for an attractive force.

The first term in Eq. (4) is the *classical* force, pictured in Fig. 1*i*. This term does not involve relativistic retardation and only requires to solve the background equation of motion. When for instance $A(\phi) = y\phi$, $V(\phi) = \frac{1}{2}m^2\phi^2$, one recovers exactly the Yukawa force (note one can use $\langle \phi \rangle(x) = y \int d^4x' i\Delta(x, x')J(x')$) giving the same result as in [22].

The second term in Eq. (4) is the *quantum* force, pictured in Fig. 1*ii*. It can be obtained by taking the derivative ∂_L of the functional determinant obtained in the explicit evaluation of $E[J]$,

$$E[J] \supset -\frac{i}{2} \text{Tr} \log(\partial^2 + V'' + A''J), \quad (6)$$

then recognizing the geometric series of insertions corresponding to the Green function satisfying Eq. (5). Alternatively, one can expand $\langle A(\phi) \rangle = A(\phi_{\text{cl}}) + \frac{1}{2}A''(\phi_{\text{cl}})\langle \eta^2 \rangle(x) + O(\hbar^2)$ and realise that $\langle \eta^2 \rangle(x)$ has to

be the connected correlator for η in presence of the source term.

The vacuum energy (in)famously contains infinities which usually have to be subtracted by hand (see *e.g.* [23, 24]). In our approach all divergences automatically disappear thanks to the ∂_L as they are L -independent, as should be the case as $\partial_L E[J]$ is an observable. Indeed, in the functional determinant, the ∂_L removes all diagrams which do not link a source to the other one, *i.e.* the “tadpole” diagrams of the extended sources, pictured in Fig. 1*iii*. Thus in Eq. (4) the infinite part of $\Delta(x, x)$ (which is L -independent) does not contribute and one can readily use its finite part $\Delta^{\text{fin}}(x, x)$ [25].

THE CHAMELEON QUANTUM FORCE

Computing the quantum force (Eq. (4)) requires to calculate the Δ_J propagator. However some important general properties can be deduced prior to any calculation. Whenever the source term $A''J$ is large with respect to other scales involved in the interaction potential, the Green’s function should vanish (*i.e.* be “screened”) inside the source and vanish at its surface, as illustrated in Fig. 1*iv*. These are precisely the conditions of the standard Casimir effect.

In the opposite limit, when the coupling to the source $A''J$ can be treated perturbatively, the functional determinant Eq. (6) can be truncated at quadratic order, in which case it is the limit of no screening where the force is

$$\begin{aligned} F_{\text{quant}} &= \frac{i}{2} \int d^4x \int d^4x' \\ &A''(x)\partial_L J(x)\Delta_0(x, x')A''(x')J(x')\Delta_0(x', x). \end{aligned} \quad (7)$$

This corresponds to the bubble diagram shown in Fig. 1*v*, which is precisely the Casimir-Polder force integrated over extended sources. For point sources $J(x) = \delta^{(3)}(x^i) + \delta^{(3)}(x^i + L^i)$, $|L^i| = L$, we obtain the potential $V_{\text{CP}}(L) = -A''(0)A''(L)\frac{1}{32\pi^3}\frac{V''}{L^2}K_1(2V''L)$. This is a generalisation of the Casimir-Polder potential in the presence of an unscreened scalar, which matches results of Refs. [26, 27] when taking $A(\phi) = \frac{\phi^2}{2M}$ and $V(\phi) = \frac{m^2}{2}\phi^2$.

The chameleon-like models are effective theories whose predictions are valid below a cutoff scale, specific to each experimental situation. When self-interactions such as $\mathcal{L} \supset \phi^n/\Lambda^{n-4}$ are present, the cutoff is expected to be $\sim 4\pi\Lambda$ since higher order diagrams are expected to produce fast-growing $1/(\Lambda L)^n$ contributions to the force which cannot be neglected when $L \sim 1/4\pi\Lambda$. The cutoff resulting from the interactions with matter is more subtle because of screening. Consider the contributions to the force from a leading interaction $M^{-2}\phi^2J$ and the next-to-leading interaction $M^{-4}\phi^4J$ (shown in Fig. 1*vi*), which contributes at two-loop as $M^{-2} \int d^4x \partial_L J(\Delta(x, x))^2$. We

obtain that the two loop contribution is negligible for

$$\Delta_J^{\text{fin}}(x_{bd}, x_{bd}) \ll M^2. \quad (8)$$

In the presence of screening, one has $\Delta_J^{\text{fin}}(x_{bd}, x_{bd}) \rightarrow 0$, and therefore the cutoff tends to infinity. This is not surprising as the Casimir pressure should not depend on the coupling to the plates, only on the mass and degrees of freedom of the field living between the plates. Also, this screening is a familiar effect in compact extra-dimension theories [28]: a large brane mass term repels the field and amounts to a Dirichlet boundary condition [29, 30]. Yet, it is remarkable that the presence of screening reduces the contributions from $n > 1$ -loop diagrams, hence improving on the \hbar expansion.

Our conclusions about the validity of the chameleon-like EFT differ from those drawn in Ref. [31] for the following reason. The reasoning of Ref. [31] would hold if the source occupied the whole space. However one should take into account that whenever an empty region exists, the fluctuation gets confined there when the effective mass induced by the source becomes large (as pictured in Fig. 1*iv*). As a consequence the contributions to the 1-loop potential in the source region are suppressed by the vanishing wave function of the fluctuation, and the chameleon-like EFT is not violated – even when the effective mass induced by the source becomes infinite.

QUANTUM FORCE BETWEEN PLATES

We now study the case of a chameleon-like field in an environment whose constant density changes piecewise along the direction z , which means the mass of the chameleon is a piecewise constant along z . This case is important as it is a sensible approximation whenever the profile of ϕ_{cl} near the interfaces is irrelevant compared to the distance L . This approximation is especially accurate for symmetron models [32].

Let us consider the case of 3 regions, for which the effective mass $V_J'' \equiv m^2(z)$ takes the form

$$m^2(z) = m_1^2 \Theta(z < 0) + m_2^2 \Theta(0 < z < L) + m_3^2 \Theta(L < z). \quad (9)$$

This can be readily used to calculate the chameleon pressure between plates of homogeneous mass density ρ , in which case m_2^2 is seen as the intrinsic mass and the sources in regions 1, 3 are identified with $M^{-2} J_{1,3} = (M)^{-2} \rho_{1,3} = m_{1,3}^2 - m_2^2$.

Defining $\omega(z) = \sqrt{|p^{0\dots 2}|^2 + i\epsilon - m^2(z)}$, the equations of motion become $(\partial_z^2 + \omega^2(z))\phi(z) = 0$. The solution in regions $i = 1, 2, 3$ is simply $(\phi_i^+, \phi_i^-) = (e^{i\omega_i z}, e^{-i\omega_i z})$. The solution everywhere can be found by continuity of the solution and its derivative at each of the interfaces, defining momentum-dependent transfer matrices of the form $(\phi_2^+, \phi_2^-)^t = T_{21}(\phi_1^+, \phi_1^-)^t$, $(\phi_3^+, \phi_3^-)^t = T_{32}T_{21}(\phi_1^+, \phi_1^-)^t$. The Feynman propagator solves $(\partial_z^2 +$

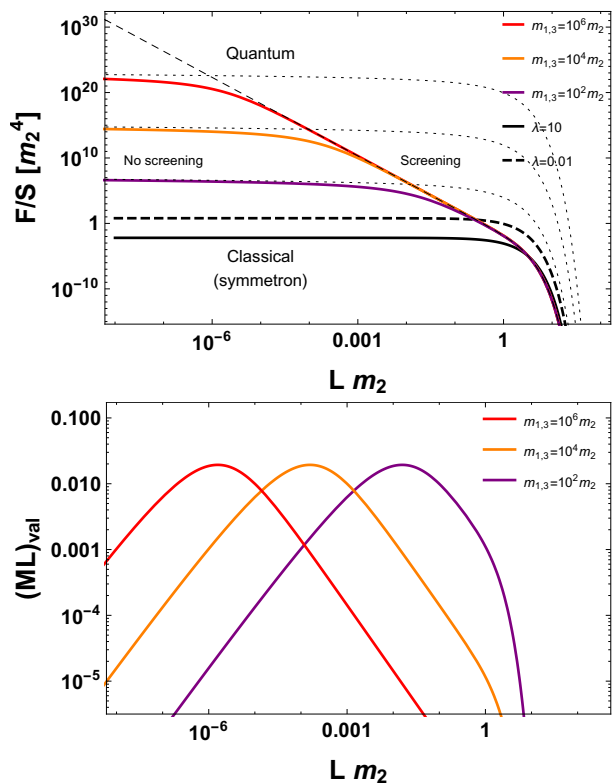


FIG. 2. Top: The quantum pressure between plates as a function of L for fixed m_2 (or vice-versa). Thin dashed line shows the Casimir pressure for a massive scalar. Thin dotted lines show the integrated Casimir-Polder force. The exact result interpolates between these two regimes. The classical pressure in the symmetron model where $m_2^2 = 2\mu^2$ is also shown. Bottom: Lower bound on ML needed for the perturbative expansion to be valid.

$\omega^2(z))\Delta_p(z, z') = -i\delta(z - z')$ with the requirement that the solution vanishes at $z = \pm\infty$.

The quantum force induced by the fluctuation between regions 1 and 3 is obtained by varying $E[J]$ with respect to L , as described in Eq. (4). The variation of the source gives a Dirac delta function at $z = L$. Moreover the source is taken to vanish near infinity at z_∞ , hence the variation of the source is $A''\partial_L J = (m_2^2 - m_3^2)(\delta(z - L) - \delta(z - z_\infty))$.

The quantity $\Delta_p(L, L) - \Delta_p(z_\infty, z_\infty)$ then appears, with

$$\Delta_p(L, L) = \frac{(\omega_1 + \omega_2) + e^{2iL\omega_2}(\omega_2 - \omega_1)}{(\omega_1 + \omega_2)(\omega_2 + \omega_3) - e^{2iL\omega_2}(\omega_2 - \omega_1)(\omega_2 - \omega_3)} \quad (10)$$

and $\Delta_p(z_\infty, z_\infty) = 1/(\omega_2 + \omega_3)$. The final expression for the pressure between regions 1 and 3 is

$$\frac{F_{\text{quant}}}{S} = \int_0^\infty \frac{d\rho\rho^2}{2\pi^2} \frac{\gamma_2(\gamma_2 - \gamma_1)(\gamma_2 - \gamma_3)}{e^{2L\gamma_2}(\gamma_1 + \gamma_2)(\gamma_2 + \gamma_3) - (\gamma_2 - \gamma_1)(\gamma_2 - \gamma_3)} \quad (11)$$

where one has performed a Wick rotation and introduced $\omega_i = i\gamma_i = i\sqrt{\rho^2 + m_i^2}$.

Let us consider some limiting cases. For $m_{1,3} \rightarrow \infty$, the expression gives the Casimir pressure from a massive scalar,

$$\frac{F_{\text{quant}}}{S} = \int_0^\infty \frac{d\rho\rho^2}{2\pi^2} \frac{\gamma_2}{e^{2L\gamma_2} - 1} \quad (12)$$

which is $\pi^2/(480L^4)$ if $m_2 = 0$.

On the other hand, weak coupling is defined by $(m_{1,3}^2 - m_2^2)/m_2^2 \ll 1$ in which case a perturbative expansion is possible. The leading order in the expansion is quadratic and gives

$$\frac{F_{\text{quant}}}{S} = (m_1^2 - m_2^2)(m_3^2 - m_2^2) \int_0^\infty \frac{d\rho\rho^2}{2\pi^2} \frac{e^{-2L\gamma_2}}{16(\gamma_2)^3}. \quad (13)$$

This corresponds exactly to the Casimir-Polder force integrated over regions 1 and 3.

Although the limits taken above are conceptually simple, the transition between both as a function of L is non trivial, as shown in Fig. 2. We see that the transition occurs over 3 orders of magnitude in L and takes place near $L \sim 1/m_{1,3}$. Qualitatively, this is the typical distance for which the chameleon-like fluctuation has high enough momentum to start travelling in the 1, 3 regions. This behaviour can be seen as a validity cutoff on the Casimir pressure, in the sense that at close enough distance the pressure becomes constant instead of keeping growing.

The validity cutoff of the prediction in the presence of a higher-dimensional coupling to matter is shown in Fig. 2. The minimum value allowed for ML , defined as $(ML)_{\text{val}} \equiv L\sqrt{\Delta_J^{\text{fin}}(x_{\text{bd}}, x_{\text{bd}})}$ following Eq. (8), reaches a maximal value of ~ 0.02 , which is similar to $\sim 1/4\pi$. This corresponds to the *lowest* possible cutoff. Conversely, in the screened regime, the cutoff tends to be much higher and goes to infinity when $m_{1,3}/m_2 \rightarrow \infty$.

QUANTUM FORCE IN THE EÖT-WASH EXPERIMENT

The torsion pendulum Eöt-Wash experiment is sensitive to many modified gravity models, it is thus interesting to evaluate the quantum force from a chameleon-like field in this setup. We use, as above, the piecewise constant mass approximation for the chameleon-like fluctuations. In this experiment an electrostatic shielding sheet is placed between the plates, thus the particle propagates in 5 different regions. The 5-layer propagator is obtained using the method described in this Letter, and the subsequent change in force is shown in Fig. 3 for a massless particle. We see that when the sheet is dense enough, it screens the propagation and the force is *enhanced* by a

factor 16, as the pressure is now between the plate and the sheet, twice closer than the opposite plate. In the screening limit of the sheet the Casimir pressure is found to be $\pi^2/(30(L + W_{\text{sheet}})^4)$ ($L = 55 \mu\text{m}$, $W_{\text{sheet}} = 10 \mu\text{m}$ for Eöt-Wash [20]).

Interestingly, without the sheet, the $L = 55 \mu\text{m}$ Eöt-Wash measurement is already close to be sensitive to the Casimir pressure induced by a chameleon-like particle. Once the effect of the sheet is taken into account, the pressure is enhanced and Eöt-Wash then becomes sensitive to such chameleon Casimir pressure.

QUANTUM BOUNDS ON CHAMELEON-LIKE MODELS

Here are the implications for two well-known models for which the piecewise constant mass approximation can be safely used.

Standard chameleon. The standard chameleon potential is

$$V_J(\phi) = \frac{\Lambda^{4+n}}{\phi^n} + e^{\frac{\phi}{M}} J. \quad (14)$$

and has been studied in great details [33, 34]. Focussing on $n = 1$, the chameleon mass between plates is found to be $m_2 \approx \pi/L$. We find that the most precise Casimir force experiments [35–37] are sensitive to the small extra Casimir pressure induced by the chameleon. It turns out that exclusions from classical and quantum forces are complementary, and the quantum force excludes a large region inaccessible to other experiments, as shown in Fig. 3.

Symmetron. The symmetron model relies on a Z_2 symmetry restoration in the presence of matter and is usually realised as

$$V_J(\phi) = \frac{1}{2} \left(\frac{1}{M^2} J - \mu^2 \right) \phi^2 + \frac{\lambda}{4} \phi^4. \quad (15)$$

The classical symmetron force between plates is suppressed and is approximated by $F_{\text{cl}} = \frac{\mu^4}{4\lambda} e^{-2\mu L}$ [22]. As made clear in Fig. 2, the classical force is suppressed with respect to the quantum one by $\sim (\mu L)^4/\lambda$ which is small at distances $L < 1/\mu$, for which the forces become active.

A simple bound on the symmetron comes from molecular spectroscopy [26, 27], in which case the Casimir-Polder force between nuclei is unscreened. At masses below the meV (see Fig. 2 in [27]), the main bound on the symmetron comes from the Eöt-Wash experiment.

Interestingly the Eöt-Wash experiment is sensitive to the symmetron Casimir pressure *because of* the intermediate shield. The $L = 55 \mu\text{m}$ measurement excludes a large part of the symmetron parameter space as shown in Fig. 3. A sensitivity up to $M \sim 1 \text{ TeV}$ and to $\mu \sim 58 \text{ meV}$ is obtained. In comparison, the classical exclusion region

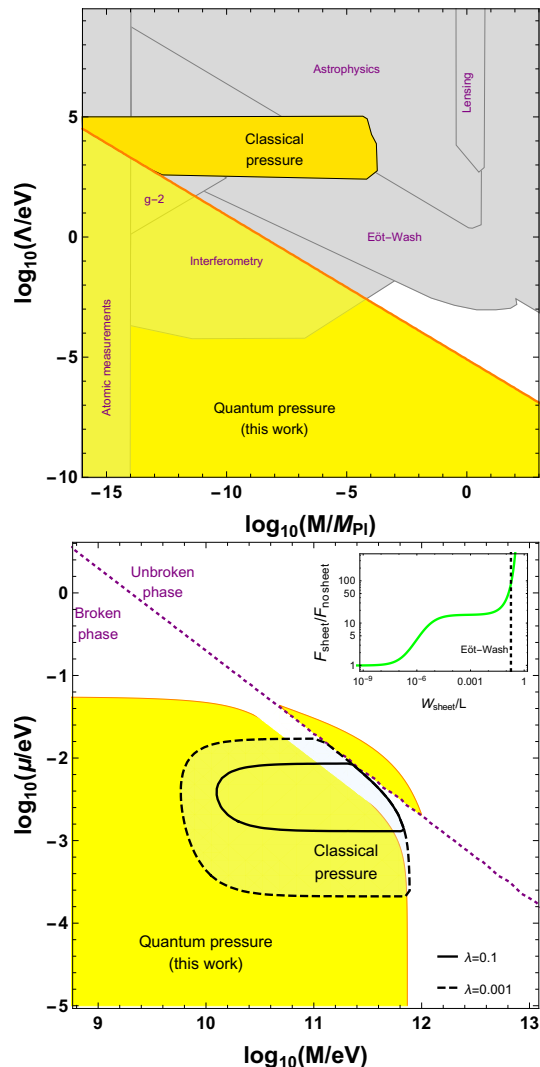


FIG. 3. Bounds on chameleon-like models. Top: Exclusion regions on the standard chameleon with $n = 1$, including bounds from Casimir experiments on the quantum and classical chameleon pressures. Bottom: Exclusion regions on the symmetron from Eöt-Wash on quantum and classical torques in presence of the intermediate sheet. Insert: Enhancement of the quantum force from an intermediate sheet as a function of its width.

[22, 38] is finite, depends on λ and vanishes for $\lambda \gtrsim 0.4$. The exclusion region near the transition requires a treatment of the VEV profile at the interface which is beyond the piecewise constant mass approximation used here.

CONCLUSION

We have studied the forces induced by chameleon-like particles in a fully-fledged quantum approach. Our formalism elucidates the role of screening in the quantum picture and naturally interpolates between the limits of Casimir and Casimir-Polder pressures. We have com-

puted propagators with piecewise constant masses in an arbitrary number of 1D regions and analyzed in details the quantum chameleon pressure between plates. Our conclusions relative to the validity of the chameleon EFT differ from [31] and are less restrictive. In the Eöt-Wash experiment we find that the sensitivity to the quantum pressure from chameleon-like fields is enhanced by the presence of the intermediate sheet. For both symmetron and standard chameleon models, the bounds on the quantum pressure exclude large and previously unconstrained regions of the parameter spaces.

ACKNOWLEDGEMENTS

SF thanks Orsay University for hospitality and funding. This work is supported by the São Paulo Research Foundation (FAPESP) under grants #2011/11973, #2014/21477-2 and #2018/11721-4. This work is supported in part by the EU Horizon 2020 research and innovation programme under the Marie-Sklodowska grant No. 690575. This article is based upon work related to the COST Action CA15117 (CANTATA) supported by COST (European Cooperation in Science and Technology).

REFERENCES

-
- * philippe.brax@ipht.fr, sylvain@ift.unesp.br
- [1] P. Brax, *Class. Quant. Grav.* **30**, 214005 (2013).
 - [2] B. Bertotti, L. Iess, and P. Tortora, *Nature* **425**, 374 (2003).
 - [3] J. G. Williams, S. G. Turyshev, and D. Boggs, *Class. Quant. Grav.* **29**, 184004 (2012), arXiv:1203.2150 [gr-qc].
 - [4] J. Khoury and A. Weltman, *Phys.Rev.Lett.* **93**, 171104 (2004), arXiv:astro-ph/0309300 [astro-ph].
 - [5] J. Khoury and A. Weltman, *Phys. Rev.* **D69**, 044026 (2004), arXiv:astro-ph/0309411.
 - [6] P. Brax, C. van de Bruck, A.-C. Davis, J. Khoury, and A. Weltman, *Phys. Rev.* **D70**, 123518 (2004), arXiv:astro-ph/0408415.
 - [7] P. Brax, C. van de Bruck, D. F. Mota, N. J. Nunes, and H. A. Winther, *Phys. Rev.* **D82**, 083503 (2010), arXiv:1006.2796 [astro-ph.CO].
 - [8] M. Pietroni, *Phys.Rev.* **D72**, 043535 (2005), arXiv:astro-ph/0505615 [astro-ph].
 - [9] K. A. Olive and M. Pospelov, *Phys. Rev.* **D77**, 043524 (2008), arXiv:0709.3825 [hep-ph].
 - [10] K. Hinterbichler and J. Khoury, *Phys. Rev. Lett.* **104**, 231301 (2010), arXiv:1001.4525 [hep-th].
 - [11] P. Brax and G. Pignol, *Phys. Rev. Lett.* **107**, 111301 (2011), arXiv:1105.3420 [hep-ph].
 - [12] T. Jenke *et al.*, *Phys. Rev. Lett.* **112**, 151105 (2014), arXiv:1404.4099 [gr-qc].

- [13] H. Lemmel, P. Brax, A. N. Ivanov, T. Jenke, G. Pignol, M. Pitschmann, T. Potocar, M. Wellenzohn, M. Zawisky, and H. Abele, *Phys. Lett.* **B743**, 310 (2015), arXiv:1502.06023 [hep-ph].
- [14] G. Cronenberg, P. Brax, H. Filter, P. Geltenbort, T. Jenke, G. Pignol, M. Pitschmann, M. Thalhammer, and H. Abele, *Nature Phys.* **14**, 1022 (2018).
- [15] C. Burrage and E. J. Copeland, *Contemp. Phys.* **57**, 164 (2016), arXiv:1507.07493 [astro-ph.CO].
- [16] M. Jaffe, P. Haslinger, V. Xu, P. Hamilton, A. Upadhye, B. Elder, J. Khoury, and H. Mller, *Nature Phys.* **13**, 938 (2017), arXiv:1612.05171 [physics.atom-ph].
- [17] P. Brax, C. van de Bruck, A.-C. Davis, D. F. Mota, and D. J. Shaw, *Phys. Rev.* **D76**, 124034 (2007), arXiv:0709.2075 [hep-ph].
- [18] P. Brax, C. van de Bruck, A. C. Davis, D. J. Shaw, and D. Iannuzzi, *Phys. Rev. Lett.* **104**, 241101 (2010), arXiv:1003.1605 [quant-ph].
- [19] A. Almasi, P. Brax, D. Iannuzzi, and R. I. P. Sedmik, *Phys. Rev.* **D91**, 102002 (2015), arXiv:1505.01763 [physics.ins-det].
- [20] E. G. Adelberger, B. R. Heckel, S. A. Hoedl, C. D. Hoyle, D. J. Kapner, and A. Upadhye, *Phys. Rev. Lett.* **98**, 131104 (2007), arXiv:hep-ph/0611223 [hep-ph].
- [21] Our conventions follow the ones of [39].
- [22] P. Brax and A.-C. Davis, *Phys. Rev.* **D91**, 063503 (2015), arXiv:1412.2080 [hep-ph].
- [23] S. Weinberg, *Rev. Mod. Phys.* **61**, 1 (1989), [,569(1988)].
- [24] K. A. Milton, *Phys. Rev.* **D68**, 065020 (2003), arXiv:hep-th/0210081 [hep-th].
- [25] In practice, it can be necessary to take a ∂_L which is slightly finite throughout the calculation.
- [26] S. Fichet, *Phys. Rev. Lett.* **120**, 131801 (2018), arXiv:1705.10331 [hep-ph].
- [27] P. Brax, S. Fichet, and G. Pignol, *Phys. Rev.* **D97**, 115034 (2018), arXiv:1710.00850 [hep-ph].
- [28] P. Brax, C. van de Bruck, and A. C. Davis, *JCAP* **0411**, 004 (2004), arXiv:astro-ph/0408464 [astro-ph].
- [29] M. Carena, T. M. P. Tait, and C. E. M. Wagner, *Acta Phys. Polon.* **B33**, 2355 (2002), arXiv:hep-ph/0207056 [hep-ph].
- [30] M. Carena, E. Ponton, T. M. P. Tait, and C. E. M. Wagner, *Phys. Rev.* **D67**, 096006 (2003), arXiv:hep-ph/0212307 [hep-ph].
- [31] A. Upadhye, W. Hu, and J. Khoury, *Phys. Rev. Lett.* **109**, 041301 (2012), arXiv:1204.3906 [hep-ph].
- [32] P. Brax and M. Pitschmann, *Phys. Rev.* **D97**, 064015 (2018), arXiv:1712.09852 [gr-qc].
- [33] C. Burrage and J. Sakstein, *JCAP* **1611**, 045 (2016), arXiv:1609.01192 [astro-ph.CO].
- [34] P. Brax, A.-C. Davis, B. Elder, and L. K. Wong, *Phys. Rev.* **D97**, 084050 (2018), arXiv:1802.05545 [hep-ph].
- [35] M. Bordag, *Advances in the Casimir Effect*, International Series of Monogr (OUP Oxford, 2009).
- [36] R. S. Decca, D. Lopez, E. Fischbach, G. L. Klimchitskaya, D. E. Krause, and V. M. Mostepanenko, *Eur. Phys. J.* **C51**, 963 (2007), arXiv:0706.3283 [hep-ph].
- [37] R. S. Decca, D. Lopez, E. Fischbach, G. L. Klimchitskaya, D. E. Krause, and V. M. Mostepanenko, *Phys. Rev.* **D75**, 077101 (2007), arXiv:hep-ph/0703290 [hep-ph].
- [38] A. Upadhye, *Phys. Rev. Lett.* **110**, 031301 (2013), arXiv:1210.7804 [hep-ph].
- [39] M. E. Peskin and D. V. Schroeder, *An introduction to quantum field theory* (Westview, Boulder, CO, 1995).

Supplemental Material

1 Casimir-Polder force between plates

In the Letter, the Casimir-Polder force between plates Eq. (13) has been obtained as the unscreened limit of the general result Eq. (11), which is given by the path integral approach introduced in this work. Here we present an alternative calculation of the Casimir-Polder force between plates, done by first calculating the Casimir-Polder force between pointlike sources using the Feynman diagram approach and then integrating over the plates. The result matches the unscreened limit Eq. (13) obtained in the Letter.

Rewrite the source term as

$$\mathcal{L} \supset A'' J(x) = \frac{1}{2} m_2^2 \eta^2 + \frac{1}{2} \eta^2 (\Theta(x < 0)(m_1^2 - m_2^2) + \Theta(r < x)(m_3^2 - m_2^2)). \quad (1)$$

We consider the presence of the plates as small perturbations, related to the coupling to individual nucleons via

$$(m_i^2 - m_2^2) = \frac{\rho_i}{\Lambda^2} = \frac{m_N n_i}{\Lambda^2} = \frac{m_N N_i}{V_i \Lambda^2} \quad (2)$$

where ρ_i is mass density, n_i is number density, N_i is the total number of particles homogeneously distributed in the volume V_i .

We first compute the potential between two point sources (the single static nucleons), replacing ρ by $m_N \delta^{(3)}(x)$. The corresponding source term is

$$\mathcal{L} \supset A J(x) = \frac{1}{2} \eta^2 \left(\frac{m_N}{\Lambda^2} \delta^{(3)}(x^i - x_a^i) + \frac{m_N}{\Lambda^2} \delta^{(3)}(x^i - x_b^i) \right). \quad (3)$$

The bubble diagram is

$$i\mathcal{M} = -\frac{m_N^2}{\Lambda^4} 4m_N^2 \frac{1}{2} \int \frac{dk^3}{(2\pi)^3} \frac{e^{i\omega_2|z_1-z_2|}}{2\omega_2} \frac{e^{i\omega'_2|z_1-z_2|}}{2\omega'_2} \quad (4)$$

where $\omega_2 = \sqrt{k^2 - m_2^2}$, $\omega'_2 = \sqrt{(k+p)^2 - m_2^2}$. In this formalism k, p are 3-momenta, $k = (k^0, k^1, k^2)$ for example. The scattering potential is given by

$$\tilde{V}(p, z_1 - z_2) = -\frac{\mathcal{M}}{4m_N^2} = -i \frac{m_N^2}{\Lambda^4} \frac{1}{2} \int \frac{dk^3}{(2\pi)^3} \frac{e^{i\gamma_2|z_1-z_2|}}{2\omega_2} \frac{e^{i\omega'_2|z_1-z_2|}}{2\omega'_2}. \quad (5)$$

The sources are static hence p_0 can readily be set to zero. The spatial potential is given by the Fourier transform of this,

$$V\left(\sqrt{(z_1 - z_2)^2 + x_{\parallel}^2}\right) = \int \frac{d^2 p_{\parallel}}{(2\pi)^2} \tilde{V}(p_{\parallel}, z_1, z_2) e^{ip_{\parallel} \cdot x_{\parallel}} \quad (6)$$

where $x_{\parallel} = (x^1, x^2)$. We are also going to average the potential over plates with separation L ,

$$V_{\text{plates}} = N_1 V_1^{-1} N_3 V_3^{-1} \int d^2 x_{\parallel} \int_{-\infty}^0 dz_1 \int d^2 x'_{\parallel} \int_L^{\infty} dz_2 \int \frac{d^2 p_{\parallel}}{(2\pi)^2} \tilde{V}(p_{\parallel}, z_1, z_2) e^{ip_{\parallel} \cdot x_{\parallel}} \quad (7)$$

where V_1, V_3 are the volumes of regions 1 and 3. One has $\int d^2 x'_{\parallel} = S$. We can see that the integrals simplify since

$$\int d^2 x_{\parallel} \frac{d^2 p_{\parallel}}{(2\pi)^2} e^{ip_{\parallel} \cdot x_{\parallel}} F(p_{\parallel}) = F(0). \quad (8)$$

Thus the potential is simply

$$V_{\text{plates}} = S n_1 n_3 \int_{-\infty}^0 dz_1 \int_L^{\infty} dz_2 \tilde{V}(0, z_1, z_2) \quad (9)$$

$$= -i S n_1 n_3 \frac{m_N^2}{\Lambda^4} \frac{1}{2} \int \frac{dk^3}{(2\pi)^3} \int_{-\infty}^0 dz_1 \int_L^{\infty} dz_2 \frac{e^{i2\omega_2(z_2 - z_1)}}{4\omega_2^2} \quad (10)$$

$$= S n_1 n_3 \frac{m_N^2}{\Lambda^4} \int \frac{dk_E^3}{(2\pi)^3} \int_{-\infty}^0 dz_1 \int_L^{\infty} dz_2 \frac{e^{-2\gamma_2(z_2 - z_1)}}{-8(\gamma_2)^2} \quad (11)$$

$$= -S n_1 n_3 \frac{m_N^2}{\Lambda^4} \int \frac{dk_E^3}{(2\pi)^3} \frac{e^{-2\gamma_2 L}}{32(\gamma_2)^4} \quad (12)$$

$$= -S(m_1^2 - m_2^2)(m_3^2 - m_2^2) \frac{m_N^2}{\Lambda^4} \int \frac{dk_E^3}{(2\pi)^3} \frac{e^{-2\gamma_2 L}}{32(\gamma_2)^4} \quad (13)$$

In the last line one has used $\frac{n_i m_N}{\Lambda^2} = m_i^2 - m_2^2$. The potential is indeed negative. Finally the pressure is obtained by taking the derivative,

$$P = S^{-1} \partial_L V_{\text{plates}} = (m_1^2 - m_2^2)(m_3^2 - m_2^2) \int \frac{dk_E^3}{(2\pi)^3} \frac{e^{-2\gamma_2 L}}{16(\gamma_2)^3}. \quad (14)$$

This reproduces Eq. (13) of the Letter.